Quaternary Science Reviews
December 2015, Volume 129 Pages 296-307
https://doi.org/10.1016/j.quascirev.2015.10.007
https://archimer.ifremer.fr/doc/00496/60725/

Mid to late Holocene strengthening of the East Greenland Current linked to warm subsurface Atlantic water

Perner Kerstin [1, *], Moros Matthias [1], Lloyd Jeremy M. [2], Jansen Eystein [3, 4], Stein Ruediger [5]

[1] Leibniz Inst Balt Sea Res, Dept Marine Geol, D-18119 Rostock, Germany.
[2] Univ Durham, Dept Geog, Durham DH1 3HP, England.
[3] Bjerknes Ctr Climate Res, Bergen, Norway.
[4] Univ Bergen, Dept Earth Sci, N-5020 Bergen, Norway.
[5] Helmholtz Ctr Polar & Marine Res, Alfred Wegener Inst, Berlin, Germany.

* Corresponding author : Kerstin Perner, email address : kerstin.pemer@io-wamemuende.de

Abstract :

The relatively fresh and cold East Greenland Current (EGC) connects the Arctic with the subpolar North Atlantic Ocean. Its strength and influence on the freshwater balance in the North Atlantic affects both the Subpolar Gyre dynamics and deep convection in the Labrador Sea. Enhanced freshwater and sea-ice expansion in the subpolar North Atlantic is suggested to modify the northward heat transport within the North Atlantic Current. High-resolution palaeoceanographic reconstructions, based on planktic and benthic foraminifera assemblage data, from the central East Greenland shelf (Foster Bugt) reveal distinct centennial to millennial-scale oceanographic variability that relates to climatic changes during the mid to late Holocene (the last c. 6.3 ka BP). Our data highlight intervals of cooling and freshening of the polar surface EGC waters that accompany warming in the subsurface Atlantic waters, which are a combination of chilled Atlantic Intermediate Water (AIW) from the Arctic Ocean and of the Return Atlantic Current (RAC) from the West Spitsbergen Current (WSC). Mid Holocene thermal optimum conditions prevailed until c. 4.5 ka BP. A thin/absent surface Polar Water layer, low drift/sea-ice occurrence and strong contribution of recirculating warm Atlantic waters at the subsurface, suggest a relatively weak EGC during this period. Subsequently, between 1.4 and 4.5 ka BP, the water column became well stratified as the surface Polar Water layer thickened and cooled, indicating a strong EGC. This EGC strengthening parallelled enhanced subsurface chilled AIW contribution from the Arctic Ocean after C. 4.5 ka BP, which culminated from 1.4 to 2.3 ka BP. This coincides with warming identified in earlier work of the North Atlantic Current, the Irminger Current, and the West Greenland Current. We link the enhanced contribution of chilled Atlantic Water during this period to the time of the 'Roman Warm Period'. The observed warming offshore East Greenland, centred at c. 1.8 ka BP, likely occurred in response to changes in the interactions of i) a weakened Subpolar Gyre; ii) increased northward heat advection in the North Atlantic Current, and iii) a predominant positive North Atlantic and Arctic Oscillation mode, prevailing during the time of the Roman Warm Period.

Highlights

► High-resolution planktic/benthic foraminiferal record from the core of the EGC. ► From 4.5 ka BP strengthening/expansion of the EGC flow. ► Parallelled by enhanced contribution AIW from the Arctic Ocean. ► Maximum AIW flow, centred at 2.0 ka BP, suggests subsurface warming. ► Subsurface warming occurs simultaneous to distinct warming in the North Atlantic.

Keywords : Foraminifera, East Greenland Current, Return Atlantic Current, Subpolar gyre, Polar front, Subpolar north Atlantic, Mid to late Holocene

1. Introduction

The East Greenland Current (EGC), a cold and low-salinity surface water current, exits the Arctic Ocean in western Fram Strait and spreads cold-water fluxes southward through Denmark Strait into the Subpolar Gyre, subsequently to the Labrador Sea and finally into the eastern North Atlantic Ocean. Potentially, an excess of cold-water fluxes can lead to a slowdown or shutdown of the Atlantic Meridional Overturning Circulation (e.g., Rahmstorf and Ganopolski, 1999; Delworth and Dixon, 2000; Clark et al., 2002). There are also indications that the strength of freshwater outflow is linked to both the strength of the North Atlantic Current (NAC) (Sundby and Drinkwater, 2007) and to deep convection in the Labrador Sea (Häkkinen and Rhines, 2004; Hansen and Østerhus, 2000; Hátún et al., 2005). Enhanced fluxes of cold freshwater of a Great Salinity Anomaly (GSA)-type event has been shown to lead to changes in the North Atlantic circulation, i.e., Subpolar Gyre dynamics (Otterå and Drange, 2004; Sundby and Drinkwater, 2007; Thornalley et al., 2009).

Palaeoceanographic studies from the North Atlantic region suggest that similar cold-spells, as seen during the GSAs, occurred during the mid to late Holocene, such as during the Little Ice Age (LIA) and the '2.7 ka BP cooling event', (e.g., Giraudeau et al., 2004; Moros et al., 2012). However, there is also evidence of pronounced shifts in climate conditions starting earlier in the Holocene from *c.* 6 to 5 ka BP, related, for example, to the Arctic Oscillation (AO) and North Atlantic Oscillation (NAO) pattern (O'Brien, 1995; Alley et al., 1999; Bakke et al., 2008), to changes in Subpolar Gyre circulation (Thornalley et al., 2009), to shifts in the current/water mass fronts (e.g.,

Rasmussen et al., 2002; Moros et al., 2012), and to glacial advance in Greenland and Scandinavia (e.g., Funder et al., 2011a; Nesje et al., 2004). Marine proxy records across the North Atlantic basin reveal opposite east-to-west trends during the late Holocene. Indeed, records located within the Northwest Atlantic Ocean indicate late Holocene (last 3.5 ka BP) cooling and enhanced southward advection of freshwater and drift/sea ice (e.g., Koç et al., 1993; Eiríksson et al., 2004; Giraudeau et al., 2004; Hall et al., 2004; Moros et al., 2006a,b, 2012; Sarafanov et al., 2009; Jennings et al., 2002, 2011; Ólafsdóttir et al., 2010; Perner et al., 2011; Telesiński et al., 2014a). In contrast, sites located within the Northeast Atlantic Ocean record a longer-term warming trend or relatively stable conditions during the late Holocene (e.g., Risebrobakken et al., 2003; Andersen et al., 2004b; Came et al., 2007; Farmer et al., 2008; Thornalley et al., 2009; Miller et al., 2011).

Sediment records from the central East Greenland shelf are ideally located to investigate the mid to late Holocene evolution of the EGC and thus the freshwater and drift/sea-ice export from the Arctic Ocean into the North Atlantic region. However, few palaeoceanographic studies from the East Greenland shelf, north of Denmark Strait, are available (e.g., Stein et al., 1993, 1996; Nam and Stein, 1999; Müller et al., 2012), due to the low phytoplankton productivity and carbonate dissolution and thus a lack of high-resolution undisturbed Holocene sediment records along the shelf (García et al., 2012). Here we present, high-resolution Holocene planktic and benthic foraminiferal assemblage data from site PS2641 from the central East Greenland shelf at 73°N. From this site, Müller et al. (2012) recently published a lower resolution record of the sea-ice proxy IP_{25}. Planktic and benthic foraminiferal abundance data allow the reconstruction of surface EGC and subsurface Atlantic Water mass characteristics over the last *c.* 6.3 ka BP. For this purpose, we use i) planktic foraminifera to investigate changes in the cold and fresh Polar Water surface layer properties and ii) benthic

foraminifera to investigate changes in the subsurface warm and saline Atlantic waters. These reconstructions provide a new perspective on the relatively poorly studied palaeoceanographic evolution of the East Greenland shelf. This new record is then compared with published key records from the North Atlantic region to provide a broader context of changes in the eastern subpolar North Atlantic region.

2. Oceanographic settings and study area

The study area (73°N and 19°W) is located on the East Greenland shelf directly below the flow path of the East Greenland Current (EGC) in Foster Bugt, a wide embayment at the mouth of the Kejser Franz Joseph Fjord (Fig. 1). Sediment core PS2641 was obtained from a sedimentary basin, landwards from a mid-shelf moraine that was deposited around 14 ka BP (Evans et al., 2002). Phytoplankton productivity is generally low in the study area due to the presence of cold and low salinity surface waters from the EGC. The EGC flows southwards along the eastern Greenland margin and is a major conduit that ventilates the North Atlantic through Denmark Strait (Fig. 1; e.g., Strass et al., 1993; Mauritzen, 1996; Rudels et al., 2002, 2005).

Today, the study site is influenced by EGC waters, which consists of an upper Polar Water layer (uppermost 250 m), which carries cold (*c.* 0-1°C) and low salinity (≤ 30) waters from the Arctic Ocean (Fig. 2; Aagaard and Coachman, 1968a,b; Johannessen, 1986; Hopkins, 1991). As illustrated in figure 1, today, subsurface waters are influenced by overflowing Atlantic Water that originates to a varying extent from Arctic Ocean Atlantic Intermediate Water (AIW; T: ≥0°C, S: 34-35; Rudels et al., 2005) and the Return Atlantic Current (RAC) from the West Spitsbergen Current (WSC, Gladfelder, 1964; T: <2°C, S: 34-35; see Fig. 2). These two water masses merge at about 78°N and are difficult to separate at our location as they move southward on the East Greenland shelf (e.g., Quadfasel et al., 1987; Rudels et al., 2005; de Steur et al.,

134 2014). However, observations by Rudels et al. (2012) show that the contribution of
135 chilled Atlantic waters from the Arctic Ocean to the East Greenland shelf was much
136 stronger in 1998 compared to in 2010. A strong halocline (at *c.* 250 m water depth)
137 forms between the surface Polar Water and the subsurface Atlantic Water and
138 produces a stable stratification (Fig. 2; Aagaard and Coachman, 1968a; Rudels, et al.,
139 2000).

140 The EGC is about 150 to 200 km wide and transports drift/sea ice, and
141 freshwater through Fram Strait via the Transpolar Drift from the Arctic Ocean into the
142 subpolar North Atlantic. Surface water currents, such as the EGC, are driven by
143 atmospheric circulation, which consequently influences the distribution of drift/sea ice
144 and water masses (Rodwell, et al., 1999; Deser et al., 2000). Under the influence of
145 northerly winds, surface Polar Water and drift/sea ice advance along the East
146 Greenland margin. Within the study area, the Polar Front represents the eastward limit
147 of perennial sea ice cover and its location during summer months depends on the
148 outflow of drift/sea-ice export from the Arctic Ocean via Fram Strait along the East
149 Greenland coast. During years of reduced summer outflow from the Arctic Ocean the
150 Polar Front retreats north-westwards from our core site, while during winter months
151 and periods of increased drift/sea-ice flow the Polar Front migrates to the south-east
152 of Foster Bugt (Pedersen et al., 2011). Variations in the strength of the Transpolar Drift,
153 and therefore drift ice and Polar Water input, is likely controlled by changes in the Arctic
154 Oscillation (AO) pattern (e.g., Kwok, 2000; Mysak, 2001). A series of prominent periods
155 of enhanced arctic freshwater and drift-ice export have been recorded in the late 1960s
156 to early 1970s, 1980s and 1990s, known as the Great Salinity Anomalies (GSA) (e.g.,
157 Dickson et al., 1988; Aagaard and Carmack, 1989; Häkkinen, 1993; Belkin et al., 1998;
158 Belkin, 2004). Freshwater pulses migrate from the Arctic Ocean downstream into the
159 subpolar North Atlantic through the EGC, eventually merging with the Jan Mayen

Current (at *c.* 74°N) and the East Icelandic Current (at c. 70°N). The East Icelandic Current flows eastwards along the North Iceland shelf and contributes freshwater to the Subpolar Gyre, thereby affecting the gyre circulation strength (e.g., Hátún et al., 2005). During times of a 'GSA' event, freshening and cooling of sea surface temperatures (SST) occurred within the North Atlantic region, shifting the Polar/Subpolar Front and consequently the maximum extent of drift ice and freshwater south-eastwards (Dooley et al., 1984; Dickson et al., 1988).

3. Material and Methods

A large box core (LBC-PS2641-5, 49.5 cm depth) and gravity core (GC-PS2641-4, 6 m depth) were obtained during ARK-X-/2 cruise with RV *Polarstern* in 1995 (Huberten, 1995), at core site PS2641 (73°09.3 N and 19°28.9 W, 469 m water depth) in Foster Bugt on the central East Greenland Shelf (Fig. 1). In this study, we focus on the uppermost 3 m of Holocene sediment.

Accelerator mass spectrometry (AMS) radiocarbon (^{14}C) dates on mollusc shells and a mix of benthic foraminifera (Table 1, Fig. 2) provide age control. In this study, we supplement the published age model by Müller et al. (2012) with additional AMS ^{14}C dates. The composite record (LBC and GC; last *c.* 6.3 ka BP) now comprises of 24 AMS ^{14}C dates. AMS ^{14}C dates were calibrated using the Marine13 calibration curve (Reimer et al., 2013) in CALIB 7.0.2 software (Stuiver and Reimer, 1993). All ages are quoted in calibrated calendar years (ka BP). So far there are no estimates of reservoir ages (ΔR) available for this region. Therefore, and for comparison of distinct palaeoceanographic changes with other records from the region, we applied a marine reservoir age of 400 years (ΔR=0).

Total mercury (Hg) and ^{137}Cs analyses were performed on sediments from the short LBC core in order to identify deposition of modern (last 50-60 years) sediments.

In modern Arctic waters, a peak in ^{137}Cs is usually found at *c.* 1963 that originates from weapons testing fallout, which follows a slow decline as ^{137}Cs is augmented by reprocessing discharges (Aarkrog et al., 1999). In Arctic sediments there is also an observable increase of the total Hg content due to enhanced anthropogenic emission reported from the 1960s (Skov et al., 2004). About 100 mg of dried and ball-milled sediment was analysed for Hg content using a Direct Mercury Analyser (DMA) (MLS GmbH 2004). Measurements of ^{137}Cs were performed on a Brad Energy Reinst-Germanium Detektor (Canberra, BE3830-7500SL-RDC-6-ULB).

Fresh sediment samples of 20-40 g were taken for planktic and benthic foraminifera counts from 1 cm sample intervals. Samples were soaked in deionized water and gently sieved at 63 µm just before counting. Foraminifera were counted on a square picking tray and identified to species level under a stereomicroscope from the wet residue >63 µm in order to reduce the loss of the more fragile arenaceous species, which is caused by drying out of the sediment. For further details on foraminiferal counting refer to Perner et al. (2011, 2013a). From the combined short and long core, 330 samples were counted and 46 benthic foraminiferal species were identified, of which 15 were agglutinates and 27 were calcareous species.

4. Results

4.1 Chronology and Lithology

Sediments from Foster Bugt are composed of dark olive grey silty clay with occasional occurrence of ice rafted debris (IRD) > 1mm. We developed a combined age-depth model for the short LBC and GC core, using the information from both the Hg content and ^{137}Cs analyses and available AMS^{14}C dates (Fig. 3A). In the LBC, a distinctive increase in the ^{137}Cs and Hg profiles from 7 cm towards the top of the core marks the onset of anthropogenic emission of the 1960s. This depth is used as a

212 stratigraphic marker. The age-depth model of the LBC is based on linear interpolation
213 between 1960, as marked by the ^{137}Cs and Hg increase, and 1995, the year of core
214 retrieval. The stratigraphies of the LBC and GC were spliced together based on the
215 total benthic foraminifera per gram sediment and the overlapping AMS ^{14}C dates (Fig.
216 3). We decided to exclude two AMS dates from intervals with overall low foraminiferal
217 content (64-82 cm, 202-228 cm depth) as AMS ^{14}C dates from the top and base of
218 each interval gave similar ages (Table 1, Fig. 3B), probably due to sediment re-
219 deposition or slide activity at the core site. Sediments from our combined cores cover
220 the last 6.3 ka BP. From 4.5 to 6.3 ka BP we find an average sedimentation rate of *c.*
221 6 cm/ka that decreases in the following interval (2.4 to 4.5 ka BP) to an average of *c.*
222 4 cm/ka. For the later part of our record, from 2.4 ka BP to 1995 AD, the average
223 sedimentation rate increased to *c.* 6 cm/ka.
224
225 4.2 Foraminiferal ecology
226 At site PS2641, the content of benthic foraminifera is relatively low and varies
227 from *c.* 5 to 40 individuals/g (Fig. 3). Throughout the core, all specimens were well-
228 preserved and showed minimal evidence of post-mortem (dissolution) changes. In
229 order to address and identify changes in the water mass characteristics of the central
230 East Greenland shelf over time, we group benthic foraminifera species into
231 associations with certain species being related to specific water mass conditions.
232 Based on the environmental preferences of these species, the associations presented
233 here, are directly and/or indirectly linked to temperature and salinity (e.g., Murray,
234 1991; Rytter et al., 2002; Sejrup et al., 2004; Lloyd et al., 2011). In table 2, we present
235 a list of foraminiferal species and groups along with information on environmental
236 preferences of each group with references that support species allocations.

Within the subpolar North Atlantic region, *Cassidulina neoteretis* is reported from areas fed by 'true' warm and saline Atlantic Water. A high abundance of this species is linked to the inflow of relatively warm Atlantic waters underneath cold and low salinity surface waters (e.g., Gooday and Lambshead, 1989; Slubowska et al., 2005). We therefore link abundance changes of this species to the occurrence of warm Atlantic waters on the East Greenland shelf. Additionally, we use a chilled Atlantic Water group (AIW group) to identify changes in the relative contribution of the Atlantic waters from the Arctic Ocean. This group includes the calcareous species *Islandiella norcrossi* and *Melonis barleeanus*, as well as the agglutinated species *Reophax pilulifer* (Table 2). The Arctic Water group (AW) includes the calcareous taxa *Elphidium excavatum* f. *clavata* and *Stainforthia feylingi* and the agglutinated taxa *Trochammina nana*, *Ammoglobigerina globigeriniformis*, *Recurvoides turbinatus* and *Textularia torquata*.

The planktic foraminiferal assemblage is dominated by the polar species *Neogloboquadrina pachyderm*a (s.) accounting for *c.* 90 to 100%, accompanied by low abundance (< 5%) of the subpolar species *Turborotalita quinqueloba*. At site PS2641, the overall occurrence of planktic foraminifera is relatively low, averaging *c.* 5% of the total foraminiferal assemblage. Therefore, we choose to present counts per gram sediment of both planktic species in the following discussion (i.e., number of individuals/g, Fig. 4). Abundance changes of planktic foraminifera on the East Greenland shelf region have been reported to be predominantly controlled by food availability (position of chlorophyll α maximum) and the position of the Arctic summer sea-ice margin (Hembleben et al., 1989; Hemleben and Schiebel, 2005; Pados and Spielhagen, 2014).

263 4.3 Mid to late Holocene foraminiferal assemblage changes

264 The following section presents the foraminiferal assemblage zones (FAZ) based
265 on single foraminiferal species and association trends.

266 FAZ I (*c.* 4.5 to 6.3 ka BP): This interval is characterised by highest content of
267 planktic foraminifera during the last 6.3 ka BP. We find a distinct peak centred *c.* 5.5
268 ka BP (14 individuals/g, Fig. 4) followed by a decrease to a minimum level of about
269 one individual/g. *Cassidulina reniforme* (*c.* 20-30%) and the warm Atlantic Water
270 associated *C. neoteretis* (*c.* 15-35%) dominate the basal part of our record, in co-
271 occurrence with the opportunistic AW species *E. excavatum* f. *clavata* (*c.* 20-40%, Fig.
272 4). We recognise a pronounced peak in AW species *E. excavatum* f. *clavata* (*c.* 45%),
273 alongside productivity indicator species *N. labradorica* (*c.* 20%), centred at 5.2 ka BP
274 and accompanied by reduced abundance of *C. neoteretis* (*c.* 10%) as well as *C.*
275 *reniforme* (*c.* 15%, Fig. 3).

276 FAZ II (*c.* 2.3 to 4.5 ka BP): This zone is characterised by a marked reduction
277 in the abundance of planktic foraminifera to an average of one individual/g. The
278 subpolar species *T. quinqueloba* occurs only sporadically throughout this interval (Fig.
279 4). This accompanies notably lower abundance of *C. neoteretis* (averaging 7%), while
280 the chilled Atlantic Water related species *I. norcrossi* and *M. barleeanus* gradually
281 increase (Fig. 4). This is accompanied by a moderate to high abundance of AW species
282 *E. excavatum* f. *clavata*. From *c.* 2.7 ka BP towards the end of this zone, we observe
283 increased abundance of the productivity indicator *N. labradorica* that accompanies a
284 distinct decrease in the overall foraminiferal content (Fig. 4).

285 FAZ III (*c.* 1.4 to 2.3 ka BP): Planktic foraminifera are almost absent, and we
286 record the lowest overall benthic foraminiferal content (Fig. 4). Within the benthic
287 assemblage *N. labradorica* is the dominant species, particularly in the early part of the
288 zone with peak abundance at 2.2 ka BP. *Islandiella norcrossi* (up to 25%) and *M.*

barleeanus (*c.* 35%) increase in abundance throughout the second half of this zone. In addition to this, we recognise higher abundance of the agglutinated 'chilled' AIW related species *R. pilulifer* (*c.* 6%), while the warm Atlantic Water associated species *C. neoteretis*, and the AW species *E. excavatum* f. *clavata* are notably reduced in abundance.

FAZ IV (*c.* 1.4 ka BP onwards): In this zone, the occurrence of planktic foraminifera recovers and a pronounced peak of *c.* 3 individuals/g is centred at *c.* 1.3 ka BP, followed by a decrease to an average of 1 individual/g. Benthic foraminifera display a marked assemblage change over the last millennium. From c. 1.4 ka BP onwards, the overall abundance of agglutinated species increase. Agglutinated AW species, such as *T. nana*, A. *globigeriniformis* and *T. torquata*, comprise *c.* 30% of the total assemblage (Fig. 4). This feature accompanies an overall reduced abundance of 'chilled' AIW species. In particular, we observe a pronounced decrease in the abundance of *N. labradorica*, *C. reniforme*, *I. norcrossi* and *E. excavatum* f. *clavata* after *c.* 0.3 ka BP.

5. Discussion

Our new high-resolution planktic and benthic foraminiferal record from Foster Bugt illustrates distinct mid to late Holocene millennial-scale variability of the EGC, and of the underlying subsurface Atlantic Water during the last *c.* 6.3 ka BP. In the following section, we first discuss the regional mid to late Holocene palaeoceanographic changes and then place our findings within the broader context of oceanic and climatic changes in the North Atlantic region. Planktic foraminiferal abundance data are used to draw conclusions on the variability of; i) the surface water characteristics and strength of the East Greenland Current (EGC), ii) sea-ice coverage, and iii) the location

315 of the Polar Front. Variability of the benthic foraminifera provide information on i)
316 characteristics of EGC subsurface waters, i.e., the relative contribution of Atlantic
317 waters to the East Greenland shelf and ii) changes in the stratification of the water
318 column.
319
320 **5.1 Long-term regional mid to late Holocene palaeoceanographic changes**
321 5.1.1 Mid Holocene Thermal Optimum conditions
322 The early part of the record (FAZ I; *c.* 4.5 to 6.3 ka BP) is characterised by
323 seasonal sea-ice cover and significant surface water productivity as indicated by
324 relatively high, but varying, abundance of planktic foraminifera and phytoplankton IP_{25}
325 indices (Müller et al., 2012; Fig. 5D and E). The Polar Front, which marks the extent of
326 perennial sea ice, was likely located in the Foster Bugt area, suggested by a prominent
327 peak in planktic foraminiferal abundance centred at *c.* 5.5 ka BP. Our data indicate a
328 relatively narrow flow of the EGC that is presumably confined to the west of our core
329 site on the East Greenland shelf, this supports previous findings from Koç et al. (1993).
330 Simultaneously, we identify relatively warm subsurface water conditions on the shelf,
331 as indicated by high abundance of *C. neoteretis* (Fig. 5B – red curve). The relatively
332 low abundance of chilled Atlantic Water indicator species (AIW group - *I. norcrossi* and
333 *M. barleeanus*; Fig. 5B – orange curve) supports this interpretation.
334 Our data thus points to reduced stratification of the water column, a seasonally
335 migrating Polar Front and an absent/weak halocline, due to a thin surface Polar Water
336 layer and likely an enhanced influence of the warm subsurface waters on surface water
337 conditions. This is in broad agreement with palaeoceanographic reconstructions from
338 the Greenland Sea (Koç et al., 1993; Telesiński et al., 2014a) as well as reported
339 relatively warm surface water conditions and a strong Atlantic Water inflow in eastern
340 Fram Strait (e.g., Werner et al., 2013). The warmer subsurface Atlantic Water at our

site may therefore originate from the recirculation of the West Spitsbergen Current (WSC), the Return Atlantic Current (RAC), in Fram Strait. A stronger RAC flow at this time is also supported by additional evidence along the east Greenland margin. Terrestrial studies from central East Greenland (Funder, 1978; Fredskild, 1991; Wagner and Melles, 2002; Wagner et al., 2008; Bennike and Wagner, 2013) report Holocene thermal optimum-like conditions prevailing until *c.* 4.5 ka BP within this area. Further downstream on the North Iceland shelf, low drift ice occurrence (Moros et al., 2006; Fig. 5G; Andrews, 2009) and relatively warm surface water conditions (Knudsen et al., 2004a; Justwan et al., 2008) suggest a weak flow of the East Icelandic Current during the same time interval, this is in agreement with our findings further north. Also, reduced sea-ice cover and weak Polar Water influence from the EGC is reported from the Southeast Greenland shelf at this time (e.g., Jennings et al., 2011; Andersen et al., 2012).

5.1.2 Onset of Neoglaciation

After *c.* 4.5 ka BP (FAZ II; *c.* 2.3 to 4.5 ka BP) cooling of surface waters and a south-eastward advance of the Polar Front, leading to permanent sea-ice cover, is inferred from notably reduced abundance of planktic foraminifera (Fig. 5D), as well as from increasing phytoplankton IP_{25} indices and sea ice algae abundance (Müller et al., 2012; Fig. 5E). It is likely that the shelf area received an enhanced contribution of cooler and fresher surface waters that consequently led to a thickening of the surface Polar Water layer. This surface cooling is accompanied by cooling of the subsurface Atlantic Water as indicated by a prominent decrease in abundance of *C. neoteretis* (Fig. 5B – red curve), which is gradually replaced by increasing abundance of chilled Atlantic Water species (Fig. 5B – orange curve).

Compared to the preceding interval, we infer a strengthening of the EGC. This must have led to a well-stratified water column and presumably favoured the formation of a distinct halocline between the Polar Water and Atlantic Water layer within the EGC. In line with our inferred timing of a stronger/expanded EGC, lake records from central East Greenland report distinct cooling from *c.* 4.5 ka BP (Wagner and Melles, 2002). The observed cooling of subsurface waters may result from either less recirculating Atlantic Water (RAC) and/or enhanced contribution of chilled Atlantic Water (AIW) from the Arctic Ocean to the East Greenland shelf. A simultaneous increase in AIW flow and the wider extent of surface EGC waters potentially reduced the impact of recirculating Atlantic Water in western Fram Strait. A reduction of RAC strength is supported by an overall decrease in Atlantic Water inflow to eastern Fram Strait and shelf/fjord areas of Spitsbergen after *c.* 5.5 ka BP (e.g., Hald et al., 2007; Werner et al., 2013; Aargaard-Sørensen et al., 2014; Rasmussen et al., 2014).

Surface water cooling, increased sea-ice coverage and/or reduced summer sea-ice break up is also recognized in the Greenland-Norwegian Sea and in eastern Fram Strait after *c.* 5.5 ka BP (Koç et al., 1993; Müller et al., 2012; Werner et al., 2013; Telesiński et al., 2014a, b). Drift ice and SST records from the North Iceland shelf report a stronger Arctic/Polar Water influence, after *c.* 5.5 ka BP (Fig. 5G; Moros et al., 2006a; Justwan et al., 2008). In addition, a sudden occurrence of coccolith species indicating the presence of warm and saline Irminger waters in subsurface waters, suggests an enhanced stratification of the water column by a thicker surface freshwater layer and thus strengthening of the East Icelandic Current (Andrews and Giraudeau, 2003; Giraudeau et al., 2004).

From *c.* 1.4 to 2.3 ka BP (FAZ III), minimum surface water productivity and a thick, cold and fresh surface Polar Water layer is indicated by an almost absent planktic foraminiferal fauna (Fig. 5D). The low abundance of planktic foraminifera suggests that

392 the Polar Front was likely located south of Foster Bugt. During this period Müller et al.
393 (2012) report a gradual increase in phytoplankton productivity and sea-ice algae
394 abundance based on IP_{25} data (Fig. 5E). However, the temporal resolution of the IP_{25}
395 data is too low compared to our foraminiferal proxy data to provide a sound correlation
396 at a centennial time scale. A distinct increase in abundance of chilled Atlantic Water
397 species (AIW group; Fig. 5B – orange line) indicates a cooling of subsurface waters.
398 We attribute these environmental conditions to an overall strengthened/expanded EGC
399 flow that produced a permanently stratified water column, separated by a well-
400 developed halocline from the underlying chilled Atlantic Water layer. The presence of
401 such a distinct halocline may also explain the parallel increase in the productivity
402 related species *N. labradorica* (e.g., Steinsund, 1994; Rytter et al., 2002; Fig. 5D). A
403 well-stratified water column due to a thick freshwater layer over the East Greenland
404 shelf is in line with findings from the Greenland Sea (Telesiński et al., 2014a). In
405 addition, these authors identify a subsurface temperature increase of *c.* 1.5°C and
406 reduced subsurface water ventilation from *c.* 2.5 to 1.5 ka BP, confined to the central
407 part of the Greenland Sea, which was likely caused by enhanced Atlantic Water inflow.
408 Furthermore, Werner et al. (2013) and Müller et al. (2012) report seasonally fluctuating
409 ice in eastern Fram Strait, alongside cool/fresh and productive surface waters after *c.*
410 3.2 ka.

411 At our study site, the distinct peak of chilled Atlantic Water occurred at the time
412 of the 'Roman Warm Period'. At this time, records from the North Iceland shelf indicate
413 surface warming (Justwan et al., 2008; Patterson et al., 2010), a weakened East
414 Icelandic Current/drift ice export (Moros et al., 2006; Fig. 5F) and increased abundance
415 of NAD related coccolith species (Andrews and Giraudeau, 2003; Fig. 6D). In addition,
416 records from the southeast Greenland shelf show a variable influence of EGC waters

(Sicre et al., 2008; Andresen et al., 2013) and increased Irminger Current contribution (Jennings et al., 2011).

Reoccurrence of planktic foraminifera from *c.* 1.4 ka BP (FAZ IV) indicate a less thick/extensive Polar Water layer and less severe drift/sea ice conditions compared to the preceding interval. This suggests a return to seasonal ice cover, presumably caused by sea-ice breaking up in late summer and seasonal migration of the Polar Front in the Foster Bugt area. The surface water conditions most likely became less harsh as surface productivity increased (Müller et al., 2012; Fig. 5D and E). An overall reduced contribution of chilled Atlantic Water species (AIW group) and a slight increase in *C. neoteretis* during the last millennium (Fig. 5B - red curve) supports this conclusion. It is likely that a weaker halocline was present during this period in Foster Bugt. In addition, harsher/less stable environmental conditions are suggested by an overall increase in abundance of agglutinated species, specifically of cold water associated agglutinated species (aggAW group, see Figs. 4 and 5A). The benthic foraminiferal fauna suggests a slightly weaker flow of the EGC, compared to the preceding interval. In line with previous research (e.g., Koç et al., 1993; Moros et al., 2006a; Telesiński et al., 2014a) we note that the EGC is still stronger and broader in extent compared to the interval *c.* 6.3 to 4.5 ka BP. Records located along the Southeast and West Greenland shelf report a similar timing in the increase of the agglutinated fauna during the last *c.* 1.5 ka BP (Jennings et al., 2002, 2011; Perner et al., 2011, 2013a). We argue that this increase of agglutinated taxa is not simply related to downcore taphonomic decay, but rather indicates harsher and more competitive environmental conditions, specifically during the last millennium. The causes of apparently more favourable conditions for agglutinated foraminifera, allowing them to be more competitive, is still not well understood and needs more detailed investigation.

Superimposed on the agglutinated faunal trend, a minor peak in the AIW group, centred at *c.* 1.0 ka BP, indicates a slight increase in chilled Atlantic Water (Fig. 5B – orange curve) that coincides with minor cooling of the surface Polar Water layer (Fig. 5D). This brief period of enhanced chilled Atlantic Water contribution coincides with the 'Medieval Climate Anomaly' and has been recognized on the Southeast Greenland shelf (e.g., Sicre et al., 2008; Andrews and Jennings, 2014).

5.2 Wider palaeoceanographic relevance of the EGC strengthening

Our foraminiferal assemblage-based reconstructions highlight a longer-term mid to late Holocene (last *c.* 6.3 ka BP) strengthening/expansion of the EGC that culminates at *c.* 1.8 ka BP. This parallels distinct changes in the composition of the subsurface Atlantic Water on the East Greenland shelf. The reduction in warm Atlantic Water (RAC) and gradual increase in chilled Atlantic Water (AIW) fauna, after 4.5 ka BP, likely occurs in response to an expanded and strengthened (colder) EGC.

An expanded EGC shifts the frontal system south-eastwards in the Nordic Seas, as prominently seen during the modern 'Great Salinity Anomalies' (Dooley et al., 1984; Dickson et al., 1988). This is consistent with the observed mid to late Holocene SST cooling and the salinity decrease during the onset of Neoglaciation caused by reduced summer and increased winter insolation along the North Atlantic Current (Andersen et al., 2004a, b; Calvo et al., 2002; Sachs, 2007). Coincident with this expanded EGC, studies from the Nordic Seas infer Atlantic Meridional Overturning Circulation weakening, which accompanies increased stratification of the upper ocean layer and a less ventilated subsurface during the late Holocene (e.g., Bauch et al., 2001; Sarnthein et al., 2003; Hall et al., 2004; Hald et al., 2007). The reduction of warm Atlantic Water may be attributed to reduced northward surface heat advection by the

North Atlantic Current from low latitudes into the subpolar North Atlantic region. Therefore, the WSC might have weakened during this period, and consequently recirculating warm and saline Atlantic Water (RAC) that eventually reached the East Greenland shelf might have been limited, and/or its position/latitude was located further south of Fram Strait. This in turn would allow an open passage for enhanced chilled Atlantic Water outflow from the Arctic Ocean as evident in our data and prominently seen by oceanographic observations in 1998 (Rudels et al., 2012).

The enhanced freshwater advection likely weakened the Subpolar Gyre circulation strength (e.g., Thornalley et al., 2009), and resulted in the observed contrasting oceanic trends in subsurface waters across the North Atlantic basin, i.e., cooling in the Northwest Atlantic (e.g., Koç et al., 1993; Giraudeau et al., 2004; Hall et al., 2004; Moros et al., 2006a,b, 2012; Sarafanov et al., 2009; Jennings et al., 2011; Perner et al., 2011; Telesiński et al., 2014a) and warm/stable conditions in the Northeast Atlantic region (e.g. Risebrobakken et al., 2003; Andersen et al., 2004b; Came et al., 2007; Farmer et al., 2008; Thornalley et al., 2009; Miller et al., 2011).

Superimposed on this longer-term mid to late Holocene cooling trend offshore East Greenland, we recognise millennial-scale cold-phases centred at 3.8, 3.0, 2.4, 1.9 - 1.4, 1.0, and 0.1 ka BP. Periods of severe sea ice conditions (almost absent planktic foraminifera; Fig. 5D) coincide with increased contribution of chilled Atlantic Water (increase in AIW group; Fig. 5B – orange curve) and minimum contribution of warmer Atlantic Water (*C. neoteretis*; Fig. 5B – red curve). These millennial scale phases correspond, within age-model uncertainties, to a southward shift of the Subpolar Front (Moros et al., 2012) and reduced deep convection in the Nordic Seas (e.g., Renssen et al., 2005; Telesiński et al., 2014a). Renssen et al. (2005) suggest that a reduced Nordic Sea deep convection is counterbalanced by enhanced deep

convection in the Labrador Sea, which in turn strengthens the North Atlantic Current flow.

5.2.1 The Roman Warm Period

The most prominent of the millennial-scale cycles present in our record, is the interval from 1.4 to 2.3 ka BP. This phase of maximum outflow of cold and low salinity surface water, contributing to the surface flow of the EGC, and subsurface chilled Atlantic Water is recognized in reconstructions from: North of Iceland (Andrews and Giraudeau, 2003; Giraudeau et al., 2004; Fig. 6C); the Reykjanes Ridge (Moros et al., 2012; Fig. 6B – grey line); the Vøring Plateau (Risebrobakken et al., 2003; Fig. 6B – dark line); the Barents Sea (Sarnthein et al., 2003); southeast Greenland (Jennings et al., 2002); and the West Greenland shelf (Moros et al., 2006b; Perner et al., 2011, 2013a; Fig. 6A). A warming is also seen in the temperature anomaly of the GISP2 ice core (Alley et al., 1999) alongside increased terrestrial winter precipitation in northern Norway (Bakke et al., 2008). In addition, subsurface warming is also reported from offshore West Africa (Morley et al., 2014). We propose that the phase between 1.4 and 2.3 ka BP is linked to the Roman Warm Period, a climatic anomaly that was suggested to equal modern climatic warming (e.g., Moberg et al., 2005; Mann et al., 2008; Ljungqvist et al., 2010). Strong contribution of chilled Atlantic Water from the Arctic Ocean to the East Greenland shelf likely occurred in response to combined changes in; i) Subpolar Gyre circulation dynamics, and/or ii) atmospheric circulation, i.e., NAO and AO modes during this time period. The weakened Subpolar Gyre circulation after *c.* 3.5 ka BP (Thornalley et al., 2009), especially following the cooling event/anomaly at *c.* 2.6 to 2.8 ka BP, would lead to enhanced advection of warm and saline waters from the Subtropical Gyre into the subpolar North Atlantic region (e.g., Häkkinen and Rhines, 2004). Consequently, the North Atlantic Drift and North Atlantic Currents are

519 strengthened and the northward heat transport within the northeast Atlantic increased
520 causing, within age-model uncertainties, a simultaneous subsurface warming along
521 the North Atlantic Drift/North Atlantic Current and its side braches (IC, WGC) during
522 the time of the Roman Warm Period. A change from an intermittently negative NAO/AO
523 to an overall positive mode has been interpreted from precipitation records (Nesje et
524 al., 2001), storm intensity reconstructions (Jackson et al., 2005), drift-ice/drift-wood
525 (Funder et al., 2011b; Darby et al., 2012), and lake sediment records (Olsen et al.,
526 2012), after *c.* 2.5/2.0 ka BP. In line with our data, Funder et al. (2011b) report
527 increased multi-year sea ice during the last *c.* 2.5 ka BP, which the authors link to
528 enhanced ice export from the western Arctic Ocean. A positive NAO/AO mode around
529 2.0 ka BP and strong Transpolar Drift may act as a potential mechanism that likely
530 favoured the expansion or strengthening of the EGC, which is essentially a response
531 to increased freshwater contribution to the EGC from the Arctic Ocean.

532 We suggest that the high contribution of chilled Atlantic Water to the East
533 Greenland shelf during the Roman Warm Period is largely due to the increased heat
534 advection of the North Atlantic Currents into the Arctic Ocean during this time. This
535 phase, centred on *c.* 1.8 ka BP, is an example of a large scale ocean-atmosphere
536 teleconnection between circulation in the North Atlantic, Nordic Seas and the Arctic
537 Ocean (Moros et al., 2012). However, the contribution of chilled Atlantic Water might
538 have been considerably stronger during the time of the Roman Warm Period,
539 compared to the Medieval Climate Anomaly. This provides further evidence that the
540 northward heat advection by the NAC was considerably stronger during the Roman
541 Warm Period than during the Medieval Climate Anomaly.

542

543

544

6. Summary and Conclusions

Planktic and benthic foraminiferal assemblage data record changes in the water mass composition of the East Greenland shelf during the mid to late Holocene (last *c.* 6.3 ka BP). We document mid Holocene thermal optimum-like conditions with a relatively low outflow of cold, low salinity water from the Arctic Ocean contributing to an overall weak/moderate EGC flow, and a thin and/or absent surface Polar Water layer, from *c.* 4.5 to 6.3 ka BP. This matches relatively low sea ice formation in the Arctic Ocean (e.g. Funder et al., 2011b). After *c.* 4.5 ka BP, our reconstructions highlight a progressive strengthening of the EGC flow representing an increase in freshwater/ice flux from the Arctic Ocean and the consequent south-eastward freshwater expansion substantially weakening the Subpolar Gyre circulation. In addition to the EGC strengthening, we note enhanced contribution of subsurface chilled Atlantic Water from the Arctic Ocean during this time. Between 1.4 and 2.3 ka BP the strongest EGC flow from the studied period is recorded. This coincides with a strong chilled Atlantic Water contribution and/or subsurface warming centred at *c.* 1.8 ka BP, which is likely linked to the Roman Warm Period. A similar warm phase is observed in marine records influenced by the North Atlantic Current from North Iceland, the SE and West Greenland shelf, on the Reykjanes Ridge, the Norwegian Sea, Barents Sea, Greenland Sea and eastern Fram Strait. This warming was considerably stronger than during the subsequent Medieval Climate Anomaly. Although the exact timing remains unclear, subsurface warming offshore East Greenland may relate to the warming of the North Atlantic Current, caused by the weakened Subpolar Gyre circulation.

Acknowledgements

The authors wish to thank the Deutsche Forschungsgemeinschaft (DFG) for funding the project 'GreenClime' (PE 2071/2-1) and Kerstin Perner. Furthermore, we thank Jens Matthießen and Henriette Kolling for their help during sediment sub-sampling and Anna-Lucia Buer for carrying out the manual sieving of the >150 µm fraction. For fruitful discussions, we thank Anne Jennings and Marit-Solveig Seidenkrantz. We thank two anonymous reviewers for their thorough and helpful comments to improve the manuscript.

Author contributions

K.P., M.M., J.M.L, E.J., and R.S. contributed to the interpretation of the data and wrote the manuscript. K.P. carried out countings of planktic and benthic foraminifera and developed the figures and tables for the manuscript. All authors discussed and commented on the manuscript.

References

Aagaard, K., Coachman, L.K. (1968a). The East Greenland Current north of Denmark Strait. Part I. Arctic 21, 181-200.

Aagaard, K., Coachman, L.K. (1968b). The East Greenland Current north of Denmark Strait. Part II. Arctic 21, 267-290.

Aargaard, K., Carmack, E.C. (1989). The role of sea ice and other dresh water in the Arctic circulation. Journal of Geophysical Research: Oceans 94, 14485-14489.

Aagaard-Sørensen, S., Husum, K., Hald, M., MArchitto,T., Godtliebsen, F. (2014). Sub sea surface temperatures in the Polar North Atlantic during the Holocene: Planktic foraminiferal Mg/Ca temperature reconstructions. The Holocene 24, 93-103.

Aarkrog, A., Dahlgaard, H. and Nielsen, S.P. (1999). Marine radioactivity in the Arctic: a retrospect of environmental studies in Greenland waters with emphasis on transport of 90Sr and 137Cs with the East Greenland Current. The Science of the Total Environment 237/238, p. 143.

Alley, R.B., Agustsdottir, A.M., and Fawcett, P.J. (1999). Ice-core evidence of late-Holocene reduction in North Atlantic Ocean heat transport. Geophysical Monograph 112, 301–312.

Alve, E. (1994). Opportunistic features of the foraminifer Stainforthia fusiformis (Williamson): evidence from Frierfjord, Norway. Journal of Micropalaeontology 13, 24.

Andrews, J.T. (2009). Seeking a Holocene drift ice proxy: non clay mineral variations from the SW to N-central Iceland shelf: trends, regime shifts, and periodicities. Journal of Quaternary Science 24, 664-676.

Andrews, J.T., Giraudeau, J. (2003). Multi-proxy records showing significant Holocene environmental variability: the inner N. Iceland shelf (Hunafloi). Quaternary Science Reviews 22, 175–193.

Andrews, J.T., Jennings, A.E. (2014). Multidecadal to millennial marine climate oscillations across the Denmark Strait (~66 degrees N) over the last 2000 cal yr BP. Climate of the Past 10, 325-343. DOI: 10.5194/cp-10-325-2014.

Andersen, C., Koc, N., Jennings, A.E., and Andrews, J.T. (2004a). Nonuniform response of the major surface currents in the Nordic Seas to insolation forcing: implications for the Holocene climate variability. Paleoceanography 19, DOI: 10.1029/2002PA000873.

Andersen, C., Koç, N., Moros, M. (2004b). A highly unstable Holocene climate in the subpolar North Atlantic: evidence from diatoms. Quaternary Science Reviews 23, 2155-2166.

623 Andersson, C., Risebrobakken, B., Jansen, E., and Dahl, S.O. (2003). Late
624 Holocene surface ocean conditions of the Norwegian Sea (Vöhring Plateau).
625 Paleoceanography 18, 1044.
626 Andresen, C.S., Hansen, M.J., Seidenkrantz, M.S., Jennings, A.E., Knudsen, M.F.,
627 Nørgaard-Pedersen, N., Larsen, N.K., Kuijpers, A., Pearce, C. (2013). Mid- to late-
628 Holocene oceanographic variability on the Southeast Greenland shelf. The
629 Holocene, DOI: 10.1177/0959683612460789.
630 Bauch, H.A., Erlenkeuser, H., Spielhagen, R.F., Struck, U., Matthiessen, J., Thiede, J.,
631 Heinemeier, J. (2001). A multiproxy reconstruction of the evolution of deep and
632 surface waters in the subarctic Nordic seas over the last 30,000 years. Quaternary
633 Science Reviews 20, 659-678. doi:10.1016/S0277-3791(00)00098-6
634 Bakke, J., Lie, Ø., Dahl, S.O., et al. (2008). Strength and spatial patterns of the
635 Holocene wintertime westerlies in the NE Atlantic region. Global and Planetary
636 Change 60, 28–41. doi:10.1016/j.gloplacha.2006.07.030
637 Belkin, I. M., S. Levitus, J. I. Antonov, and S.-A. Malmberg (1998). ‘‘Great Salinity
638 Anomalies’’ in the North Atlantic. Progress in Oceanography 41, 1–68.
639 Belkin, I. (2004). Propagation of the “Great Salinity Anomaly” of the 1990s around the
640 northern North Atlantic. Geophysical Research Letters 31, L08306,
641 doi:10.1029/2003GL019334.
642 Bennike, O., Wagner, B. (2013). Holocene range of *Mytilus edulis* in central East
643 Greenland. Polar Record 49, 291-296.
644 Bourke, R.H., Weigel, A.M., Paquette, R.G. (1988). The westward turning branch of
645 the West Spitzbergen Current. *Journal of Geophysical Research* **93**, 14065-14077.
646 Calvo, E., Grimalt, J., Jansen, E. (2002). High resolution Uk37 sea surface temperature
647 reconstruction in the Norwegian Sea during the Holocene. Quaternary Science
648 Reviews 21, 1385–1394.

649 Came, R.E., Oppo, D.W., McManus, J.F. (2007). Amplitude and timing of temperature
650 and salinity variability in the subpolar North Atlantic over the past 10 k.y. Geology
651 35, 315–318.
652 Caralp, M.H. (1989). Abundance of Bulimina exilis and MeIonis barleeanum:
653 relationship to the quality and quantity of organic matter. Geo-Marine Letters 9, 37-
654 43.
655 Clark, P.U., Pisias, N.G., Stocker, T.F., Weaver, A.J. (2002). The role of the
656 thermohaline circulation in abrupt climate change. Nature 415, 863-869.
657 Corliss, B.H. (1991). Morphology and microhabitat preferences of benthic foraminifera
658 from the northwest Atlantic Ocean. Marine Micropaleontology 17, 195-236.
659 Curry, R., Mauritzen, C. (2005). Dilution of the Northern North Atlantic Ocean in Recent
660 Decades. Science 308, 1772-1774. DOI: 10.1126/science.1109477
661 de Steur, L., Hansen, E., Mauritzen, C., Beszczynska-Möller, A., Fahrbach, E. (2014).
662 Impact of recirculation on the East Greenland Current in Fram Strait: Results from
663 moored current meter measurements between 1997-2009. *Deep-Sea-Research I*
664 **92**, 26-40.
665 Darby, D., Ortiz, J.D., Grosh, C.E., Lund, S. (2012). 1,500-year cycle in the Arctic
666 Oscillation identified in Holocene Arctic sea-ice drift. Nature Geoscience 5, 897-900.
667 doi:10.1038/ngeo1629.
668 Delworth T.L., Dixon, K.W. (2000). Implications of the recent trend in the Arctic/North
669 Atlantic Oscillation for the North Atlantic Thermohaline Circulation. Journal of
670 Climate 13, 3721-3427.
671 Deser, C., Walsh, J.E., Timlin, M.S. (2000). Arctic Sea Ice Variability in the Context of
672 Recent Atmospheric Circulation Trends. Journal of Climate 13, 617-633.

673 Dickson, R.R., Meincke, J., Malmberg, S.-A., Lee, A.J. (1988). The “Great Salinity
674 Anomaly” in the northern North Atlantic, 1968-1982. Progress in Oceanography 20,
675 103-151.
676 Dooley, H.D., Martin, J.H.A., Ellett, D.J. (1984). Abnormal hydrographic conditions in
677 the Northeast Atlantic during the 1970s. Rapports et Proces-Verbaux des Reunions.
678 Conseil International pour lExploration de la Mer 185, 179–187.
679 Eiríksson, J., Larsen, G., Knudsen, K.L., Heinemeier, J., S´monarson, L.A. (2004).
680 Marine reservoir age variability and water mass distribution in the Iceland Sea.
681 Quaternary Science Reviews 23, 2247-2268.
682 Erbs-Hansen, D.R., Knudsen, K.L., Olsen, J., Lykke-Andersen, H., Underbjerg, J.A.,
683 Sha, L. (2013). Paleoceanographical development off Sisimiut, West Greenland,
684 during the mid- and late Holocene: A multiproxy study. Marine Micropaleontology
685 102, 79-97.
686 Evans, J., Dowdeswell, J.A., Grobe, H., Niessen, F., Stein, R., Hubberten, H.-W.,
687 Whittington, R.J. (2002). Late Quaternary sedimentation in Kejser Franz Jospeh
688 Fjord and the continental margin of East Greenland. In: Dowdeswell, J.A., Cofaigh,
689 C.Ó. (Eds.), Glacier-influenced Sedimentation on High-Latidtude Continental
690 Margins. Geological Society, London, pp. 149-179.
691 Farmer, E.J., Chapman, M.R., Andrews, J.E. (2008). Centennial-scale Holocene North
692 Atlantic surface temperatures from Mg/Ca ratios in Globigerina bulloides.
693 Geochemistry, Geophysics, Geosystems 9, Q12029. doi:10.1029/2008GC002199.
694 Fairbanks, R. G., Wiebe, P. H., Be, A. W. H. (1980). Vertical distribution and isotopic
695 composition of living planktonic foraminifera in the western North Atlantic. Science
696 207, 61–63.
697 Funder, S. (1978). Holocene stratigraphy and vegetation history in the Scoresby Sund
698 area, East Greenland. Bulletin Grønlands Geologiske Undersøgelse 129, 66 pp.

699 Funder, S., Kjeldsen, K.K., Kjaer, K.H., Ó Cofaigh, C. (2011a). The Greenland Ice
700 Sheet during the past 300,000 years: a review. Dev. Quat. Sci. 15, 669-713.
701 Funder, S. et al. (2011b) A 10,000 year record of Arctic Ocean Sea-Ice Variability-View
702 from the Beach. Science 333, 747-750. DOI: 10.1126/science.1202760.
703 García, M., Dowdeswell, J.A., Ercilla, G., Jakobsson, M. (2012). Recent glacially
704 influenced sedimentary processes on the East Greenland continental slope and eep
705 Greenland basin. Quaternary Science Reviews 49, 64-81.
706 Giraudeau, J., Jennings, A.E., Andrews, J.T. (2004). Timing and mechanisms
707 of surface and intermediate water circulation changes in the Nordic Seas over the
708 last 10 000 cal. Years: a view from the North Iceland shelf. Quaternary Science
709 Reviews 23, 2127-2139.
710 Giraudeau, J., Grelaud, M., Solignac, S., Andrews, J. T., Moros., M., Jansen,
711 E. (2010). Millennial-scale variability on Atlantic water advection to the Nordic Seas
712 derived from Holocene coccolith concentration records. Quaternary Science
713 Reviews 29.
714 Gooday, A.J., Lambshead, P.J.D. (1989). The influence of seasonally deposited
715 phytodetritus on benthic foraminiferal populations in the bathyal northeast Atlantic:
716 the species response. Marine Ecology Progress Series 58, 53-67.
717 Häkkinen, S. (1993). An Arctic source for the Great Salinity Anomaly: A simulation of
718 the Arctic ice ocean system for 1955–1975. Journal of Geophysical Research 98,
719 16,397–16,410..
720 Häkkinen, S., Rhines, P.B. (2004). Decline of subpolar North Atlantic circulation during
721 the 1990s. Science 304, 555–559.
722 Hald, M., Dokken, T., Korsun, S., Polyak, L., Aspeli, R. (1994). Recent and
723 Late Quaternary distribution of Elphidium excavatum f. clavata in Arctic seas.
724 Cushman Foundation Special Publication 32, 141–153.

725 Hald, M., Steinsund, P.I. (1996). Benthic foraminifera and carbonate dissolution
726 in surface sediments of the Barents- and Kara Seas. Ber. Polarforsch., 21 2 (1
727 996).
728 Hald, M., Korsun, S. (1997). Distribution of modern benthic foraminifera from
729 fjords of Svalbard, European Arctic. Journal of Foraminiferal Research 27, 101-22.
730 Hald, M., Andersson, C., Ebbesen, H., Jansen, E., Klitgaard-Kristensen, D.,
731 Risebrobakken, B., Salomonsen, G. R., Sarnthein, M., Sejrup, H. P.,Telford, R. J.
732 (2007). Variations in temperature and extent of Atlantic Water in the northern North
733 Atlantic during the Holocene. Quaternary Science Reviews 26, 3423–3440. doi:
734 10.1016/j.quascirev.2007.10.005.
735 Hall, I.G., Bianchi, G., Evans, J.R. (2004). Centennial to millennial scale
736 Holocene climate-deep water linkages in the North Atlantic. Quaternary Science
737 Reviews 23, 1529– 1536.
738 Hansen, A. & Knudsen, K.L. (1995). Recent foraminiferal distribution in
739 Freemansundet and Early Holocene stratigraphy on Edgeeya. Svalbard. Polar
740 Research I4, 215-238.
741 Hansen, B,. Østerhus, S. (2000). North Atlantic-Nordic Seas exchanges. Progress in
742 Oceanography 45, 109–208.
743 Hátún, H., Sando, A. B., Drange, H., Hansen, B., Valdimarsson, H. (2005). Influence
744 of the Atlantic subpolar gyre on the thermohaline circulation. Science 309, 1841–
745 1844.
746 Hebbeln, D., Henrich, R., Baumann, K. H. (1998) Paleoceanography of the last
747 interglacial/glacial cycle in the Polar North Atlantic. Quaternary Science Reviews 17,
748 125–153.
749 Hemleben, C., Spindler, M., Anderson, O.R. (1989). Modern Planktonic Foraminifera.
750 Springer, 30 New York, 1989.

751 Henrich, R., Baumann, K.-H., Huber, R., Meggers, H. (2002). Carbonate preservation
752 records of the past 3 Myr in the Norwegian-Greenland Sea and the northern North
753 Atlantic: Implications for the history of NADW production. Marine Geology 184, 17–
754 39.
755 Hopkins, T.S. (1991). The GIN Sea - A synthesis of its physical oceanography and
756 literature review, 1972-1985.
757 Hubberten, H.-W., 1995. Die Expedition ARKTIS-X/2 mit FS Polarstern (1994). (The
758 Expedition ARKTIS-X/2 of RV Polarstern in 1994). Alfred Wegener Institute for Polar
759 and Marine Research, Bremerhaven.
760 Huber, R., Meggers, H., Baumann, K.H., Henrich, R. (2000). Recent and Pleistocene
761 carbonate dissolution in sediments of the Norwegian-Greenland Sea. Marine
762 Geology 165, 123-136.
763 Jennings, A.E., Knudsen, K.L., Hald, M., Hansen, C.V., Andrews, J.T. (2002). A mid-
764 Holocene shift in Arctic sea-ice variability on the East Greenland Shelf. The
765 Holocene 12, 49-58.
766 Jennings, A.E., Weiner, N.J., Helgadottir, G., Andrews, J.T. (2004). Modern
767 Foraminiferal fauna of the southwestern to northern Iceland shelf: oceanographic
768 and environmental control. Journal of Foraminiferal Research 34, 180-207.
769 Jennings, A.E., Andrews, J., Wilson, L. (2011). Holocene environmental evolution of
770 the SE Greenland Shelf North and South of the Denmark Strait: Irminger and East
771 Greenland current interactions. Quaternary Science Reviews 30, 980-998.
772 Johannessen, O.M. (1986). "Brief overview of the physical oceanography." In: The
773 Nordic Seas. Hurdle, B.G. (eds.). New York, Springer-Verlag, 103-1 27.
774 Jonkers L., Brummer G.-J.A., Peeters F.J.C., van Aken H.M., De Jong M.F. (2010).
775 Seasonal stratification, shell flux, and oxygen isotope dynamics of left-coiling N.

776 pachyderma (sin.) and T. quinqueloba in the western subpolar North Atlantic.
777 Paleoceanography 25, PA2204, doi: 10.1029/2009PA001849.
778 Justwan A., Koç N., Jennings A.E. (2008). Evolution of the Irminger and East Icelandic
779 current systems through the Holocene, revealed by diatom-based sea surface
780 temperature reconstructions. Quaternary Science Reviews 27, 1571–1582.
781 Kleinen, T. Osborn, T.J., Briffa, K.R. (2009). Sensitivity of climate response to
782 cariations in freshwater hosing locations. Ocean Dynamics 59, 509-521.
783 Knudsen, K.L., Søndergaard, M.K.B., Eiríksson, J., Jiang, H. (2008). Holocene thermal
784 maximum off North Iceland: Evidence from benthic and planktonic foraminifera in
785 the 8600-5200 cal year BP time slice. Marine Micropaleontology 67, 120-142.
786 Koç, N., Jansen, E., Haflidason, H. (1993). Paleoceanographic reconstructions of
787 surface ocean conditions in the Greenland, Iceland and Norwegian seas through
788 the last 14 ka based on diatoms. Quaternary Science Reviews 2, 115-140.
789 Kohfeld K.E., Fairbanks R.G., Smith S.L. & Walsh I.D. (1996). Neogloboquadrina
790 pachyderma (sinistral coiling) as palaeoceanographic tracers in polar oceans:
791 evidence from Northeast Water Polynya plankton tows, sediment traps, and surface
792 sediments. Paleoceanography 11, 679-699.
793 Korsun S. A., Polyak L. V. (1989). Distribution of benthic foraminiferal morphogroups
794 in the Barents Sea. Okeanologiya 29, 838-844.
795 Kwok, R. (2000). Recent changes in Arctic Ocean sea ice motion associated with the
796 North Atlantic Oscialltion. Geophysical Sesearch Letters 27, 775-778.
797 Levitus, S., Antonov, J.I., Boyer, T.P., Stephens, C. (2000). Warming of the World
798 Ocean. Science 287, 2225-2229. DOI: 10.1126/science.287.5461.2225
799 Lloyd, J.M., Kuijpers, A., Long, A., Moros, M., and Park, L.A. (2007). Foraminiferal
800 reconstruction of mid- to late-Holocene ocean circulation and climate variability in
801 Disko Bugt, West Greenland. The Holocene 17, 1079-1091.

802 Lloyd, J.M., Moros, M., Perner, K., Telford, R., Kuijpers, A., Jansen, E., McCarthy, D.J.
803 (2011). A 100 year record of ocean temperature control on the stability of
804 Jakobshavn Isbrae, West Greenland. Geology 39, 867-870.
805 Ljungqvist, F.C. (2010). A new reconstruction of temperature variability in the extra-
806 tropical Northern Hemisphere during the last two millennia. Geografiska Analer
807 Series A 92, 339-351.
808 Mann, M.E., Zhang, Z., Hughes, M.K., Bradley, R.S., Miller, S.K., Rutherford, S., Ni, F.
809 (2008). Proxy-based reconstructions of hemispheric and global surface temperature
810 variations over the past two millennia. Proceedings of the National Academy of
811 Sciences, USA, 105, 13252–13257.
812 Mauritzen, C., (1996). Production of dense overflow waters feeding the North Atlantic
813 across the Greenland Sea–Scotland Ridge: Part 1. Evidence for a revised
814 circulation scheme. Deep-Sea Research 43, 769–806.
815 Milller, K.R., Chapman, M.R., Andrews, J.E., Koç, N. (2011). Diatom phytoplankton
816 response to Holocene climate change in the Subpolar North Atlantic. Global and
817 Planetary Change 79, 214-225.
818 Moberg, A., Sonechkln, D.M., Holmgren, K., Datsenko, N.M. and Karlén, W. (2005).
819 Highly variable Northern Hemisphere temperatures reconstructed from low- and
820 high-resolution proxy data. Nature 433, 613–617.
821 Moros, M., Emeis, K., Risebrobakken, B., Snowball, I., Kuijpers, A., McManus,
822 J. and Jansen, E. (2004). Sea surface temperatures and ice rafting in the Holocene
823 North Atlantic: climate influences on northern Europe and Greenland. Quaternary
824 Science Reviews 23, 2113–2126.
825 Moros, M., Andrews, J.T., Eberl, D.D. and Jansen, E. (2006a). Holocene history of
826 drift ice in the northern North Atlantic: Evidence for different spatial and temporal
827 modes. Paleoceanography 21, 2017.

828 Moros, M., Jensen, K.G., Kuijpers, A. (2006b). Mid- to late-Holocene hydrographic and
829 climate variability in Disko Bugt, central West Greenland. The Holocene 16, 357–
830 367.
831 Moros, M., Jansen, E., Oppo, D., Giraudeau, J., Kuijpers, A. (2012). Reconstruction of
832 the late Holocene changes in the Sub-Arctic Front position at the Reykjanes Ridge,
833 north Atlantic. The Holocene, 22, 877-886.
834 Murray, J.W. (1991). Ecology and palaeoecology of benthic foraminifera. Longman,
835 London, 397pp.
836 Müller, J., Werner, K., Stein, R., Fahl, K., Moros, M., Jansen, E. (2012). Holocene
837 cooling culminates in sea ice oscillations in Fram Strait. Quaternary Science
838 Reviews 47, 1-14.
839 Mysak, L.A., (2001). Patterns of Arctic circulation. Science 293, 1269–1270.
840 Nam, S., Stein, R. (1999). Late Quaternary variations in sediment accumulation rates
841 and their paleoenvironmental implications: A case study from the East Greenland
842 Continental Margin. In: Bruns, P. and Hass, H. C. (Eds.), On the Determination of
843 Sediment Accumulation Rates, GeoResearch Forum Vol. 5, Trans Tech
844 Publications, 223-240.
845 Nesje, A., Matthews, J.A., Dahl, S.O, Berrisford, M.S., Andersson, C. (2001). Holocene
846 glacier fluctuations of Flatebreen and winter-precipitation changes in the
847 Jostedalsbreen region, western Norway, based on glaciolacustrine sediment
848 records. Holocene 11, 267–280.
849 O'Brien, S. R., Mayewski, P.A., Meeker, L.D., Meese, D. A., Twickler, M. S., Whitlow,
850 S.I. (1995). Complexity of Holocene climate as reconstructed from a Greenland ice
851 core. Science 270, 1962–1964.

852 Olsen, J., Anderson, J.N., Knudsen, M.F. (2012). Variability of the North Atlantic
853 Oscillation over the past 5,200 years. Nature Geoscience 5, 808-812.
854 DOI:10.1038/NGEO1589,
855 Oppo, D.W., McManus, J.F., Cullen, J.R. (2003). Palaeoceanography:
856 deepwater variability in the Holocene epoch. Nature 422, 277.
857 Osterman, L.E., Nelson, A.R. (1989). Latest Quaternary and Holocene
858 paleoceanography of the eastern Baffin Island continental shelf, Canada: benthic
859 foraminiferal evidence. Canadian Journal of Earth Science 26, 2236–2248.
860 Otterå, O.H., Frange, H. (2004). Effects of solar irradiance forcing on the ocean
861 circulation and sea-ice in the North Atlantic in an isopycnic coordinate ocean general
862 circulation model. Tellus 56A, 154-166.
863 Ólafsdóttir, S., Jennings, A. E., Geisdóttir, Á., Andrews, J., Miller, G. (2010).
864 Holocene variability of the North Atlantic Irminger current on the south- and
865 northwest shelf of Iceland. Marine Micropaleontology 77 (3-4), 101-118.
866 Pados, T., Spielhagen, R.F. (2014). Species distribution and depth habitat of recent
867 planktic foraminifera in the Fram Strait (Arctic Ocean). Polar Research 33, 224-283.
868 doi: 10.34027/polar.v33.22483
869 Patterson, W.P., Dietrich, K.A., Holmde, C., Andrews, J.T. (2010). Two millennia of
870 North Atlantic seasonality and implications for Norse colonies. PNAS 107, 5306-
871 5310. doi: 10.1073/pnas.0902522107
872 Petersen (2011) DMI, 2012 - Danish Meteorological Institute and National Snow and
873 Ice Data Center. Compiled by V. Underhill and F. Fetterer. 2012. Arctic Sea Ice
874 Charts from Danish Meteorological Institute, 1893 - 1956. [indicate subset used].
875 Boulder, Colorado USA: National Snow and Ice Data Center.
876 http://dx.doi.org/10.7265/N56D5QXC.

877 Perner, K., Moros, M., Lloyd, J.M., Kuijpers, A., Telford, R.J., Harff, J. (2011).
878 Centennial scale benthic foraminiferal record of late Holocene oceanographic
879 variability in Disko Bugt, West Greenland. Quaternary Science Reviews 30, 2815–
880 2826.
881 Perner, K., Moros, M., Jennings, A., Lloyd, J.M., Knudsen, K.L. (2013a). Holocene
882 palaeoceanographic evolution of West Greenland. The Holocene 23, 374–387.
883 Polyak, L., Solheim, A. (1994). Late- and postglacial environments in the
884 northern Barents Sea west of Franz Josef Land. Polar Research 13, 197–207.
885 Quadfasel, D., Gascardm J.C. Koltermann, K.P. (1987). Large-scale oceanography in
886 Fram Strait during the 1984 marginal ice zone experiments. Journal of Geophysical
887 Research 92, 6719-6728.
888 Rahmstorf, S., Ganopolski, A. (1999). Long-term global warming scenarios computed
889 with an efficient coupled climate model. Climate Change 43, 353-367.
890 Ran, L., Jiang, H., Knudsen, K.L., Eiríksson, J. (2008). The mid- to late
891 Holocene paleoceanographic changes in the northern North Atlantic. Front. Earth
892 Science China 1, 449-457.
893 Rasmussen, T.L., Thomsen, E., Troelstra, S.R. et al. (2002). Millenial-scale glacial
894 variability versus Holocene stability: Changes in planktic and benthic foraminifera
895 faunas and ocean circulation in the North Atlantic during the last 60,000 years.
896 Marine Micropaleontology 47, 143–176.
897 Reimer *et al*. (2013). IntCal13 and MARINE013 radiocarbon age calibration curves 0-
898 50000 years cal BP. Radiocarbon 55, azu_js_rs.55.16947.
899 Risebrobakken, B., Jansen, E., Andersson, C., Mjelde, E., and Hevroy, K. (2003).
900 A high-resolution study of Holocene paleoclimatic and paleoceanographic changes
901 in the Nordic Seas. Paleoceanography 18, 1017–1031.

902 Risebrobakken, B., Moros, M., Ivanova, E. V., Chistyakova, N., Rosenberg, R. (2010).
903 Climate and oceanographic variability in the SW Barents Sea during the Holocene.
904 The Holocene 20, 609–621. doi:10.1177/0959683609356586.
905 Rodwell, M.J., Rowell, D.P., Folland, C.K. (1999). Oceanic forcing of the wintertime
906 North Atlantic Oscillation and European climate. Nature 398, 320-323.
907 Rudels, B., Meyer, R., Fahrbach, E., Ivanov, V.V., asterhus, S., Quadfasel, D.,
908 Schauer, U., Tverberg, V., Woodgate, R.A. (2000). Water mass distribution in Fram
909 Strait and over the Yermak Plateau in summer 1997. Ann. Geophys. 18, 687– 705.
910 Rudels, B., Fahrbach, E., Meincke, J., Bude´us, G., Eriksson, P. (2002). The East
911 Greenland Current and its contribution to the Denmark Strait Overflow. ICES Journal
912 of Marine Science 59, 1133– 1154.
913 Rudels, B., Björk, G., Nilsson, J., Winsor, P., Lake, I., Nohr, C. (2005). The interaction
914 between waters from the Arctic Ocean and the Nordic Seas north of Fram Strait and
915 along the East Greenland Current: results from the Arctic Ocean-02 Oden
916 expedition. Journal of Marine Systems 55, 1-30.
917 Rudels, B., et al. (2012). The East Greenland Current and its impact on the Nordic
918 Seas: observed trends in the past decade. ICES Journal of Marine Science 69, 841-
919 851.
920 Rytter, F., Knudsen, K.L., Seidenkrantz, M.-S., Eiríksson, J. (2002). Modern
921 distribution of benthic foraminifera on the North Icelandic shelf and slope. Journal of
922 Foraminiferal Research 32, 217–244.
923 Sachs, J.P. (2007). Cooling of Northwest Atlantic slope waters during the Holocene.
924 Geophysical Research Letters 34, DOI: 10.1029/2006GL028495.
925 Sarnthein, M., van Kreveld, S., Erlenkeuser, H. et al. (2003). Centennial-to-millennial-
926 scale periodicities of Holocene climate and sediment injections off the western
927 Barents shelf, 75°N. Boreas 32, 447–461.

928 Schafer and Cole (1986)

929 Schiebel, R., Hemleben, C. (2005). Modern planktic foraminifera. Palaeontol. Z. 79,

930 135–148.

931 Sejrup, H.P., Birks, H.J.B., Klitgaard-Kristensen, D., Madsen, H. (2004). Benthonic

932 foraminiferal distributions and quantitative transfer functions for the northwest

933 European continental margin. Marine Micropaleontology, 53, 197-226.

934 Sicre, M-A., et al. (2008). Decadal variability of sea surface temperatures off North

935 Iceland over the last 2000 years. Earth and Planetary Science Letters 268, 137-142.

936 Skov, H., Christenden, J., Asmund, G., Rysgaard, S., Nielsen, T.G., Dietz, R., Riget,

937 F. (2004). Fate of mercury in the Arctic (FOMA). National Environmental Research

938 Institute, Denmark. NERI Technical Report No. 511, p. 56.

939 <http://Technicalreport.dmu.dk>.

940 Slubowska, M. A., Koç, N., Rasmussen, T. L., Klitgaard-Kristensen, D. (2005).

941 Changes in the flow of Atlantic water into the Arctic Ocean since the last

942 deglaciation: Evidence from the northern Svalbard continental margin, 80°N

943 Paleoceanography 20, PA4014, doi:10.1029/2005PA001141.

944 Stein, R., Nam, S-I, Grobe, H., and Hubberten, H. (1996). Late Quaternary glacial

945 history and short-term ice-rafted debris fluctuations along the East Greenland

946 continental margin. In. Andrews, J., Austin, W.E.N., Bergsten, H., and Jennings,

947 A.E. (Eds.), Late Quaternary Paleoceanography of the North Atlantic Margins, Geol.

948 Soc. London, Spec. Publ., 111, 135-151.

949 Stein, R., Grobe, H., Hubberten, H., Marienfeld, P., and Nam, S. (1993). Latest

950 Pleistocene to Holocene changes in glaciomarine sedimentation in Scoresby Sund

951 and along the adjacent East Greenland Continental Margin: Preliminary results.

952 Geo-Marine Letters 13, 9-16.

953 Steinsund, P.I., Polyak, L., Hald, M., Mikhailov, V., Korsun, S. (1994).

954 Distribution of calcareous benthic foraminifera in recent sediments of the Barents
955 and Kara Sea. In Steinsund, P.I., Benthic foraminifera in surface sediments of the
956 Barents and Kara Seas: modern and late Quaternary application. Ph.D. thesis,
957 Department of Geology, Institute of Biology and Geology, Univeristy of Tromsø.
958 Sundby, S., Drinkwater, K. (2007). On the mechanisms behind salinity anomaly signals
959 of the northern North Atlantic. Progress in Oceanography, 73, 190-202.
960 Telesinski, M.M., Spielhagen, R.F., Lind, E.M. (2014a). A high-resolution Lateglacial
961 and Holocene palaeoceanographic record from the Greenland Sea. Boreas 43, 273-
962 285. 10.1111/bor.12045. ISSN 0300-9483.
963 Telesinski, M.M., Spielhagen, R.F., Bauch, H.A. (2014b). Water mass evolution of the
964 Greenland Sea since late glacial times. Climate of the Past, 10, 123-136.
965 Thornalley, D.J.R., Elderfield, H., and McCave, I.N. (2009). Holocene oscillations in
966 temperature and salinity of the surface subpolar North Atlantic. Nature, 457 (5) 711-
967 714.
968 Vilks, G. (1989). Ecology of Recent foraminifera on the Canadian continental shelf of
969 the Arctic Ocean, in Herman, Y. (ed.), The Arctic Seas—Climatology,
970 Oceanography, Geology and Biology: Van Nostrand Reinhold, New York, p. 497–
971 569.
972 Volkmann, R. (2000). Planktic foraminifers in the outer Laptev Sea and the Fram Strait
973 – modern distribution and ecology. Journal of Foraminiferal Research 30, 157–176.
974 Wagner, B., Melles, M. (2002). Holocene environmental history of western Ymer Ø,
975 East Greenland, inferred from lake sediments. Quaternary International 89, 165-
976 176. DOI:10.1016/S1040-6182(01)00087-8.
977 Wagner, B., Bennike, O., Bos J.A.A., Cremer, H., Lotter A.F., Melles, M. (2008). A
978 multidisciplinary study of Holocene sediment records from Hjort Sø on Store

Koldewey, Northeast Greenland. Journal of Paleolimnology 39, 381-398. DOI: 10.1007/s10933-007-9120-3.

Werner, K., Spielhagen, R.F., Bauch, D., Hass, H.C., Kandiano, E. (2013). Atlantic Water advection versus sea-ice advances in the eastern Fram Strait during the last ka: Multiproxy evidence for a two-phase Holocene. Paleoceanography 28, 283-295.

Zamelczyk, K., Rasmussen, T.L., Husum, K., Haflidason, H., de Vernal., Ravna, E.K., Hald, M., Hillaire-Marcel, C. (2012). Paleoceanographic changes and calcium carbonate dissolution in the central Fram Strait during the last 20 ka. Quaternary Research 78, 405-416.

Figure captions

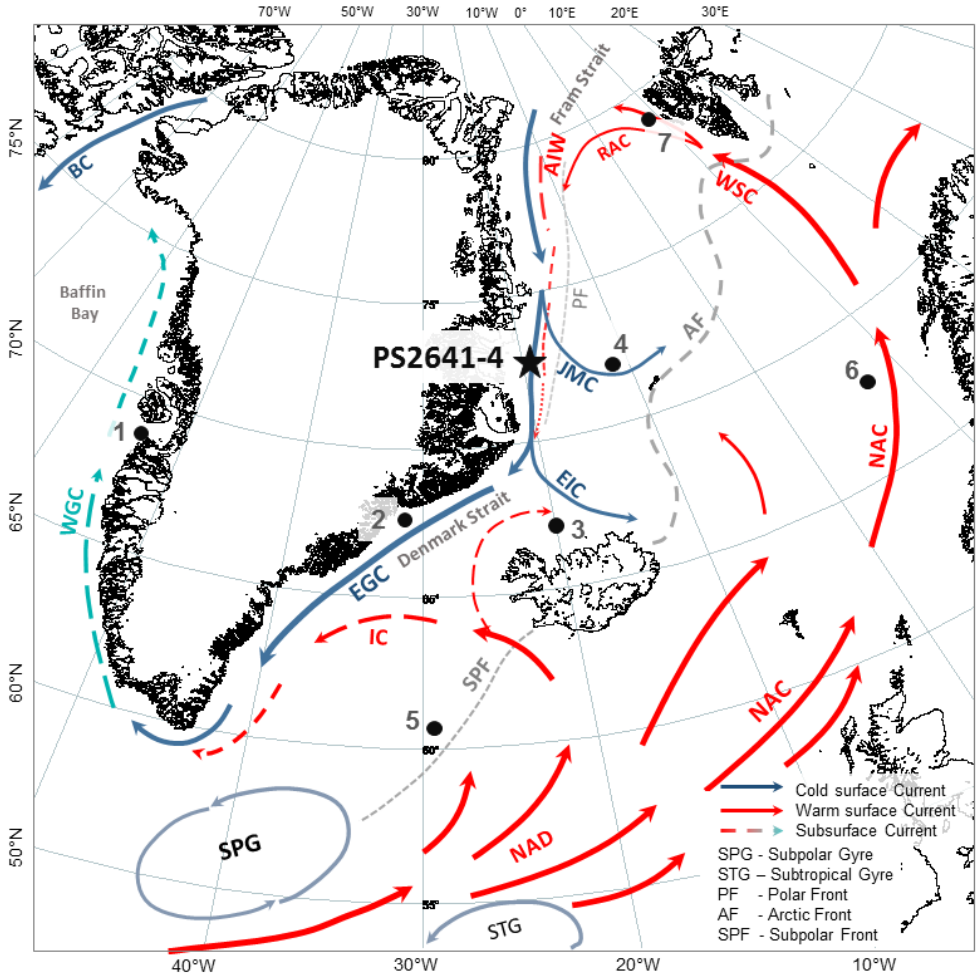

Figure 1. Map of the study area with schematic illustration of the major currents in the North Atlantic region. Abbreviations are as follows: East Greenland Current (EGC), East Icelandic Current (EIC), Jan Mayen Current (JMC), West Greenland Current (WGC), Baffin Current (BC), Irminger Current (IC), North Atlantic Current (NAC), North Atlantic Drift (NAD), West Spitzbergen Current (WSC), Return Atlantic Current (RAC). Key sites pertinent to this study: 1) West Greenland – 343310 (Perner et al., 2011); 2) SE Greenland shelf – MD2322 (Jennings et al., 2011); 3) North Iceland shelf – MD99-2269 (Andrews and Giraudeau, 2003; Moros et al., 2006a); 4) Greenland See – PS1878 (Telesiński et al., 2014a); 5) Reykjanes Ridge – DS2P (Moros et al., 2012); 6) Vøring Plateau – MD95-2011 (Risebrobakken et al., 2003); 7) Eastern Fram Strait – MSM5/5-712 (Werner et al., 2013).

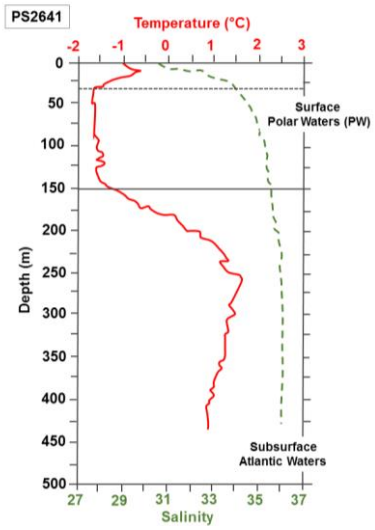

1018

1019 **Figure 2.** Temperature (red line) and salinity (green line) profile from site PS2641 in

1020 Foster Bugt, obtained during cruise ARK-X-/2 with the *Polarstern* in 1995 (Hubberten,

1021 1995).

1022

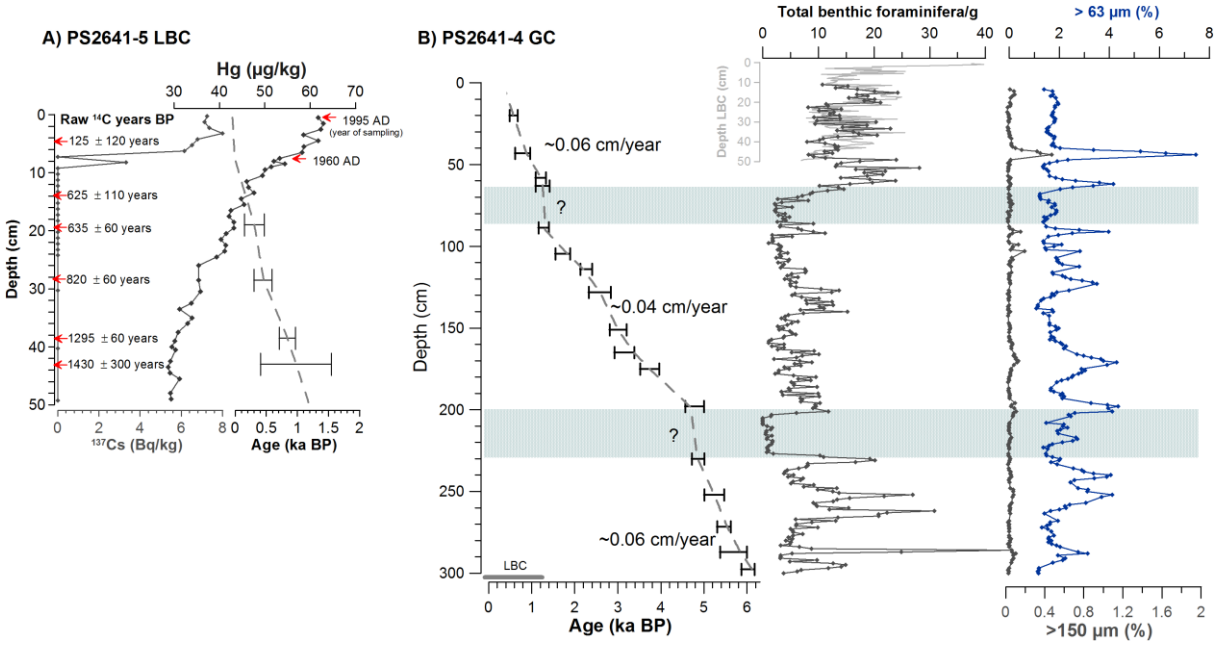

1023

1024 **Figure 3.** Age versus depth profile of cores PS2641-4 GC and PS2641-5 LBC,

1025 including AMS ^{14}C dates used for age model reconstruction. A) AMS ^{14}C dates, total

1026 Hg content and ^{137}Cs profile for the LBC. B) Sieve-fraction percentage data (>63 and

1027 >150 µm), counts of the total benthic foraminifera per gram sediment for the GC

1028 (dark line) and the LBC (grey line).

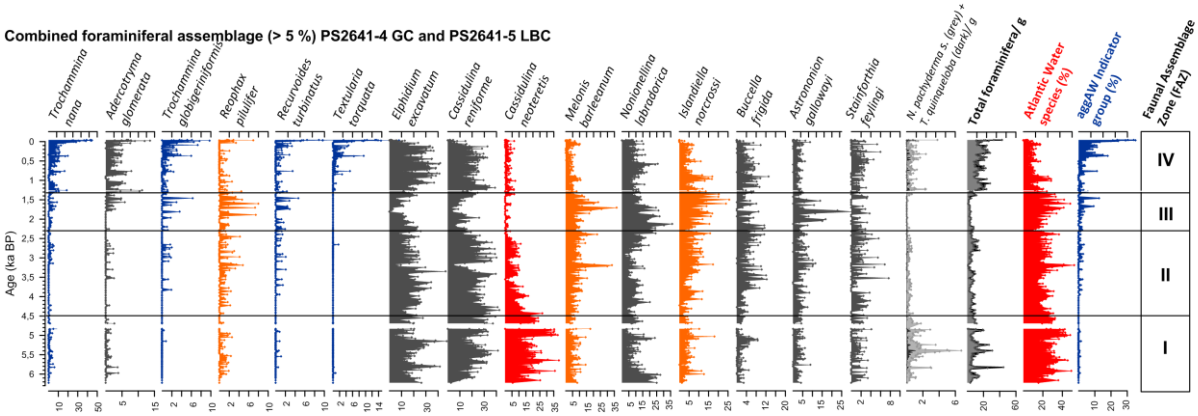

Figure 4. Percentage abundance > 5% of the total benthic foraminiferal assemblage. The content of planktic foraminifera is displayed as number of individuals counted per gram sediment. Chilled Atlantic Water (AIW) group – *I. norcrossi*, *M. barleeanus*, *R. pelulifer*; warm Atlantic Water indicator – *C. neoteretis*, agglutinated Arctic Water indicators (aggAW) – *R. recurvoides*, *A. globigeriniformis*, *T. nana*.

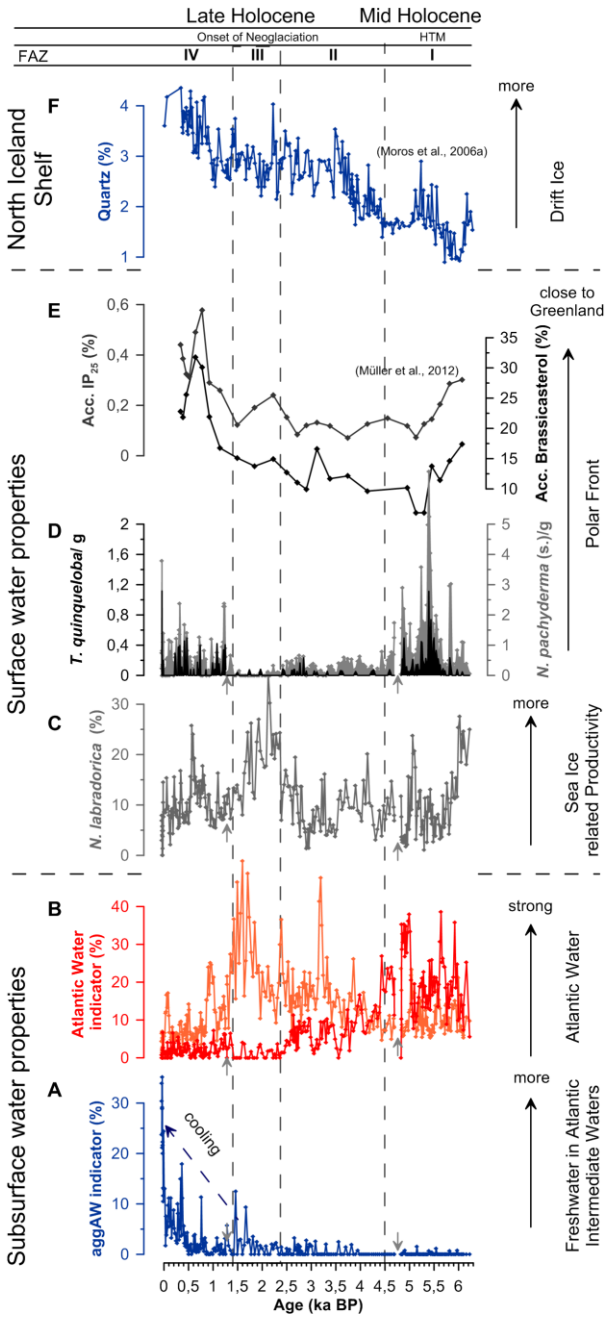

Figure 5. Regional mid to late Holocene (last *c.* 6.3 ka BP) paleoceanographic changes reconstructed from core PS2641-4GC. A) Abundance (%) of agglutinated Arctic Water species; B) Abundance (%) of warm Atlantic Water associated species *C. neoteretis*; C) Abundance (%) of the chilled Atlantic Water (AIW) group; D) Abundance (%) of *N. labradorica*; E) Content of planktic foraminifera *N. pachyderma* (s.) and *T. quinqueloba*; F) Accumulation (%) of IP_{25} and brassicasterol, phytoplankton marker from this core site, published by Müller et al. (2012); G) Drift ice proxy record (Quartz %) from North Iceland Shelf (MD99-2269, Moros et al., 2006a).

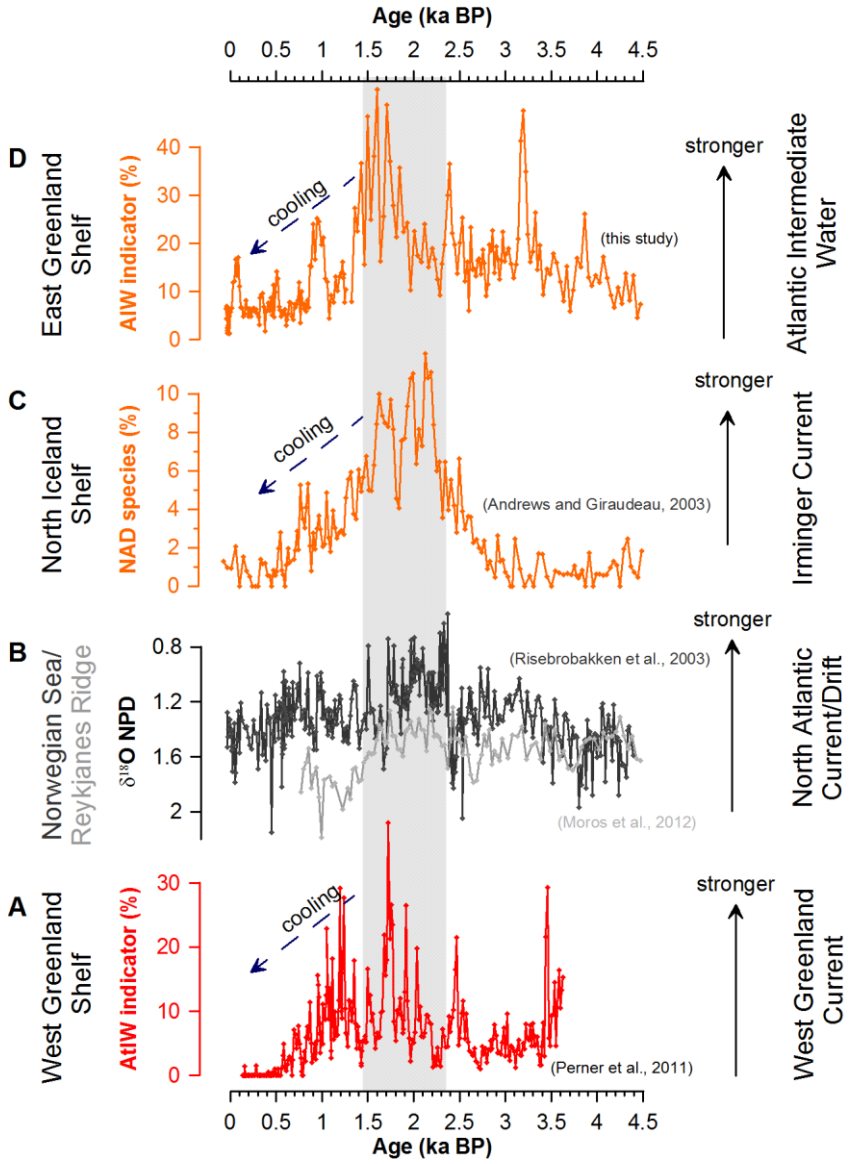

Figure 6. Palaeoceanographic changes within the subpolar North Atlantic region during the last *c.* 4.5 ka BP. A) Abundance (%) of Atlantic Water (AtlW) indicators (%) from the West Greenland shelf (red line MSM 343310, Perner et al., 2011); B) $\delta^{18}O$ of *N. pachyderma* (d.) from the Reykjanes Ridge (grey line, Moros et al., 2012) and the Norwegian Sea (dark line, Risebrobakken et al., 2003); C) North Atlantic Drift (NAD) coccolith assemblage from the North Iceland Shelf (MD99-2269, Andrews abd Giraudeau, 2003); D) chilled Atlantic Water (AIW) group (%) from East Greenland Shelf (PS2641, this study).